Empiricism Journal
https://journal-center.litpam.com/index.php/empiricism
email: empiric.journal@gmail.com

Vol. 5, No 2, Dec. 2024
e-ISSN: 2745-7613
pp. 214-223

Characterization of Crystal Structures and Magnetic Properties of Polyethylene Glycol (PEG-4000) and Silica Encapsulated $Mn_{0.5}Zn_{0.5}Fe_2O_4$ Nanoparticles

Edwin Laisina[1]*, Edi Suharyadi[2]
[1]Department of Physics, FST, Universitas Pattimura, Jl. Ir. Putuhena, Ambon, Indonesia 97233.
[2]Department of Physics, FMIPA, Universitas Gadjah Mada, Jl. Geografi, Yogyakarta, Indonesia 55281.
Email Korespondensi: edwinlaisinaugm@gmail.com

Abstract

In this research has been successfully $Mn_{0.5}Zn_{0.5}Fe_2O_4$ nanoparticles synthesis using co-precipitation method and their encapsulation by varying the concentration of polyethylene glycol (PEG-4000) and silica. The result of X-Ray Diffraction (XRD) characterization showed that $Mn_{0.5}Zn_{0.5}Fe_2O_4$ nanoparticles was mix spinel crystal structure. There was a phase other than $Mn_{0.5}Zn_{0.5}Fe_2O_4$ phase synthesized that α-Fe_2O_3 phase before and after encapsulated with PEG-4000 and silica. Encapsulation of silica has showed a new diffraction peak (222) because silica was crystal. $Mn_{0.5}Zn_{0.5}Fe_2O_4$ particle size before and after encapsulated with PEG-4000 (50% concentration) and silica (50% concentration) was 27.28±0.26 nm; 19.13±0.13 nm and 32.75±0.55 nm, respectively. The result of Transmission Electron Microscopy (TEM) characterization showed that before encapsulated with PEG-4000 and silica, occur agglomeration, meanwhile after encapsulated, the agglomeration was reduced. The result of Fourier Transform Infra Red (FTIR) characterization showed that $Mn_{0.5}Zn_{0.5}Fe_2O_4$ nanoparticles encapsulated with PEG-4000 there was shift in the wavenumbers 2878.00 cm^{-1} to 2885.51 cm^{-1} in the functional groups C-H and wavenumbers 1103.28 cm^{-1} to 1111.00 cm^{-1} in the functional groups C-O-C. Both of those functional groups was a constituent bond PEG-4000. Bonding metal oxide (M-O) was shift the wavenumbers 578.64 cm^{-1} to 570.93 cm^{-1}, which was an uniform pattern of $Mn_{0.5}Zn_{0.5}Fe_2O_4$. $Mn_{0.5}Zn_{0.5}Fe_2O_4$ encapsulated with silica was shown in the wavenumbers 1049.28 cm^{-1}; 779.24 cm^{-1}; and 471.00 cm^{-1}, which is the functional groups Si-O-Si (stretching). The characterization result of $Mn_{0.5}Zn_{0.5}Fe_2O_4$ magnetic properties with Vibrating Sample Magnetometer (VSM) showed that the values of coercivity, magnetization (at H = 15 kOe) and remnant magnetization was 47.55 Oe, 10.41 emu/g, 1.40 emu/g. After $Mn_{0.5}Zn_{0.5}Fe_2O_4$ nanoparticles encapsulated with PEG-4000 and silica was decreased amounting to 45.80 Oe, 45.64 Oe, 10.32 emu/g, 1.34 emu/g, 0.28 emu/g and 0.07 emu/g, respectively.

Keywords: *$Mn_{0.5}Zn_{0.5}Fe_2O_4$, Encapsulation, PEG-4000, Silica, Co-Precipitation.*

How to Cite: Laisina, E. & Suharyadi, E. (2024). Characterization of Crystal Structures and Magnetic Properties of Polyethylene Glycol (PEG-4000) and Silica Encapsulated $Mn_{0.5}zn_{0.5}fe_2o_4$ Nanoparticles. *Empiricism Journal*, *5*(2), 214–223. https://doi.org/10.36312/ej.v5i2.2273

https://doi.org/10.36312/ej.v5i2.2273

INTRODUCTION

Nanotechnology represents a transformative field, profoundly influencing the global economy, industrial advancements, and daily human life. One of the most actively explored domains within nanotechnology is magnetic nanoparticles, characterized by their exceptional chemical, mechanical, optical, and magnetic properties. These nanoparticles hold vast potential for applications ranging from magnetic fluids, catalysis, and bio-applications to advanced uses such as magnetic resonance imaging (MRI) and data storage technologies (Ngarajan & Hatton, 2008; Lu et al., 2007). Among magnetic nanoparticles, spinel ferrites with the general formula MFe_2O_4 (where M can be Zn^{2+}, Mn^{2+}, or Mg^{2+}) have garnered significant attention for their favorable properties, including high saturation magnetization, low coercivity, and controlled anisotropy (Mandal et al., 2002; Deraz & Alarifi, 2012).

Despite extensive research on manganese-zinc (Mn-Zn) ferrites, challenges persist in their practical application due to issues such as particle agglomeration and inconsistencies in magnetic properties. These issues not only hinder the material's magnetic performance but also limit its utility in advanced applications like magnetic hyperthermia, drug delivery systems, and contrast agents for MRI. For instance, nanoparticles often exhibit a tendency to agglomerate during synthesis, leading to increased particle sizes and non-uniform

properties (Liu et al., 2007). Addressing these challenges requires innovative surface modification and encapsulation strategies to stabilize the nanoparticles and preserve their intrinsic properties.

Encapsulation materials such as polyethylene glycol (PEG) and silica have emerged as promising solutions to mitigate these issues. PEG, a synthetic polymer, is widely recognized for its stability, biocompatibility, and ability to prevent agglomeration through steric hindrance (Zhang et al., 2005). Among PEG variants, PEG-4000 offers advantages in terms of availability, cost-effectiveness, and functional performance compared to lower molecular weight alternatives like PEG-200 or PEG-800. Its molecular structure enables effective binding with nanoparticles, reducing particle clustering and enhancing dispersion stability (Widakdo et al., 2018).

Silica, another prominent encapsulation material, is valued for its chemical stability, ease of surface modification, and ability to form uniform coatings around nanoparticles. It provides additional benefits such as increased thermal stability and compatibility with aqueous and organic solvents (Zhao et al., 2007). Importantly, silica's precursors, such as sodium silicate (Na_2SiO_3), offer a cost-effective and environmentally friendly alternative to traditional silicate precursors like tetraethyl orthosilicate (TEOS) and tetramethyl orthosilicate (TMOS). Na_2SiO_3, derived from renewable sources like plant ash, aligns with sustainability goals while minimizing toxicity and environmental impact (Ashraf et al., 2015).

While PEG and silica encapsulation have shown promise in enhancing nanoparticle stability and functionality, several limitations remain. Previous studies indicate that PEG's effectiveness as an encapsulation material can vary depending on its molecular weight and concentration. For instance, lower molecular weight PEGs may provide insufficient steric hindrance, leading to suboptimal stabilization (Kareem et al., 2016). Furthermore, the encapsulation process can alter the magnetic properties of Mn-Zn ferrites, as the introduction of non-magnetic coatings may reduce saturation magnetization and coercivity (Widakdo et al., 2018; Dabagh et al., 2023). These alterations can restrict the nanoparticles' application in areas demanding strong magnetic responses.

Additionally, the synthesis parameters, including temperature, pH, and precursor concentration, significantly influence the structural and functional outcomes of the encapsulated nanoparticles. Variability in these parameters can lead to inconsistent results, emphasizing the need for a systematic investigation of encapsulation conditions (Kareem et al., 2016). Silica encapsulation, while providing robust coatings, poses its own challenges, such as potential interference with magnetic interactions and the formation of undesirable phases under certain synthesis conditions (Dabagh et al., 2023).

The primary objective of this study is to address the persistent challenges in synthesizing high-performance $Mn_{0.5}Zn_{0.5}Fe_2O_4$ nanoparticles, focusing on mitigating particle agglomeration and maintaining magnetic properties through effective encapsulation strategies. The research aims to achieve this by synthesizing nanoparticles using the co-precipitation method and subsequently encapsulating them with varying concentrations of polyethylene glycol (PEG-4000) and silica. Through this approach, the study seeks to evaluate the impact of encapsulation on key characteristics, including particle size, crystallinity, and magnetic behavior. Additionally, the research investigates the influence of synthesis parameters such as precursor concentration and encapsulation material properties to identify optimal conditions for minimizing agglomeration and preserving magnetic functionality. By integrating these aspects, the study aspires to provide comprehensive insights into the interplay between encapsulation materials and nanoparticle performance, ultimately contributing to the development of advanced magnetic nanomaterials suitable for biomedical and industrial applications.

By systematically examining the interplay between encapsulation materials, synthesis conditions, and nanoparticle properties, this study seeks to advance the understanding of encapsulation strategies for Mn-Zn ferrites. The findings are expected to contribute to the development of high-performance magnetic nanoparticles for biomedical and industrial applications.

The novelty of this research lies in its dual focus on addressing agglomeration and preserving magnetic properties through controlled encapsulation. Unlike previous studies that often prioritize one aspect over the other, this study adopts a holistic approach,

integrating advanced characterization techniques such as X-ray diffraction (XRD), Fourier-transform infrared spectroscopy (FTIR), and vibrating sample magnetometry (VSM) to provide comprehensive insights into the structural, functional, and magnetic transformations induced by encapsulation.

Moreover, the use of Na_2SiO_3 as a sustainable silica precursor underscores the environmental relevance of this study. By highlighting the advantages and challenges associated with Na_2SiO_3 based encapsulation, this research aligns with the growing emphasis on green chemistry and sustainable materials in nanotechnology.

METHOD

PEG-4000 and Silica encapsulated nanoparticle $Mn_{0.5}Zn_{0.5}Fe_2O_4$ were prepared by two step for each encapsulation materials. Firstly, $Mn_{0.5}Zn_{0.5}Fe_2O_4$ were prepared by the coprecipitation method. In the second step, for PEG-4000 encapsulation by varying concentration and use precursor Na_2SiO_3, and for silica encapsulation also by varying concentration. XRD patterns were recorded on Shimadzu XD-3D using CuK_α radiation. FTIR transmission spectra were taken using FTIR spectrometer Shimadzu Prestige-21. Magnetic properties were studied by using Vibrating Sample Magnetometer (VSM) Riken Denshi Co.Ltd.

Preparation of Magnetic Nanoparticle

Nanoparticle $Mn_{0.5}Zn_{0.5}Fe_2O_4$ were prepared by coprecipitation method. The main ingredients of the synthesis are The stoichiometric amouts of 2.703 g $FeCl_3.6H_2O$ (Merck, Germany) were dissolved in 25 ml aquades, 0.508 g $MgCl_2.6H_2O$ (Merck, Germany) and 0.594 g $NiCl_2.6H_2O$ (Merck, Germany) were also dissolved in 25 ml aquades and then 3.37 ml HCl added. The solution then added dropwise to 10 M NaOH (Merck, Germany) solution. The reaction was kept under constant stirring at 90˚C for 1 h. Precipitated ferrite nanopowder were washed with aquades for 6 times. Finally, sample were dried on furnace at 95˚C for 5 hrs.

$Mn_{0.5}Zn_{0.5}Fe_2O_4$+PEG-4000 Nanoparticles

Nanoparticle $Mn_{0.5}Zn_{0.5}Fe_2O_4$ dissolved to 10 mL PEG-4000 solution with varying concentration (Tabel 2). PEG-4000 solution were prepared by add PEG-4000 to aquades stirring at room temperature for 30 minutes. Then, 0.6 g powder $Mn_{0.5}Zn_{0.5}Fe_2O_4$ added to PEG-4000 solution and stirring at room temperature for 1 h. Finally, sample were dried at room temperature.

Tabel 1. Sample $Mn_{0.5}Zn_{0.5}Fe_2O_4$ with varying concentration PEG-4000

Sample	$Mn_{0.5}Zn_{0.5}Fe_2O_4$: PEG-4000	PEG-4000 Concentration
A	3:1 (0,6 g : 0,2 g)	25%
B	2:1 (0,6 g : 0,3 g)	33%
C	1:1 (0,6 g : 0,6 g)	50%
D	1:2 (0,6 g : 1,2 g)	67%
E	1:3 (0,6 g : 1,8 g)	75%
F	1:4 (0,6 g : 2,4 g)	80%

Silica Encapsulated $Mg_{0.5}Ni_{0.5}Fe_2O_4$ Nanoparticles

Nanoparticle $Mn_{0.5}Zn_{0.5}Fe_2O_4$ dissolved to 30 ml silica solution with varying concentration (Tabel 1). Silica solution were prepared by add Na_2SiO_3 to aquades stirring at room temperature for 30 minutes. Then, 0.6 g powder $Mn_{0.5}Zn_{0.5}Fe_2O_4$ added to silica solution and stirring at room temperature for 5 h. encapsulated ferrite were washed with aquades for 5 times. Finally, sample were dried at room temperatur and then dried on furnace at 50˚C for 30 minutes.

Table 2. Sample $Mn_{0.5}Zn_{0.5}Fe_2O_4$ with varying concentration Silica

Sample	$Mn_{0.5}Zn_{0.5}Fe_2O_4$: Silica solution
P	0.6 g : 50% (15 mL SS + 15 mL aquades)
Q	0.6 g : 30% (9 mL SS + 21 mL aquades)
R	0.6 g : 20% (6 mL SS + 24 mL aquades)
S	0.6 g : 15% (4.5 mL SS + 25.5 mL aquades)

Sample	$Mn_{0.5}Zn_{0.5}Fe_2O_4$: Silica solution
T	0.6 g : 10% (3 mL SS + 27 mL aquades)
U	0.6 g : 5% (1.5 mL SS + 28.5 mL aquades)

RESULT AND DISCUSSION

$Mn_{0.5}Zn_{0.5}Fe_2O_4$+PEG-4000 nanoparticles

Figure 1 shows the XRD patterns of $Mn_{0.5}Zn_{0.5}Fe_2O_4$ nanoparticles before and after encapsulation with PEG-4000. The patterns shows the peak characteristics as (220), (311), (400), (511), and (440) according to JCPDS (no: 10-0467) was mix spinel crystal structure. The peaks of $Mn_{0.5}Zn_{0.5}Fe_2O_4$ encapsulation results in a relatively small shift toward the left. This is due to a uniform strains and indicates the expansion of lattice parameters. Then again, also formed α-Fe_2O_3 phase (Modak et al., 2008).

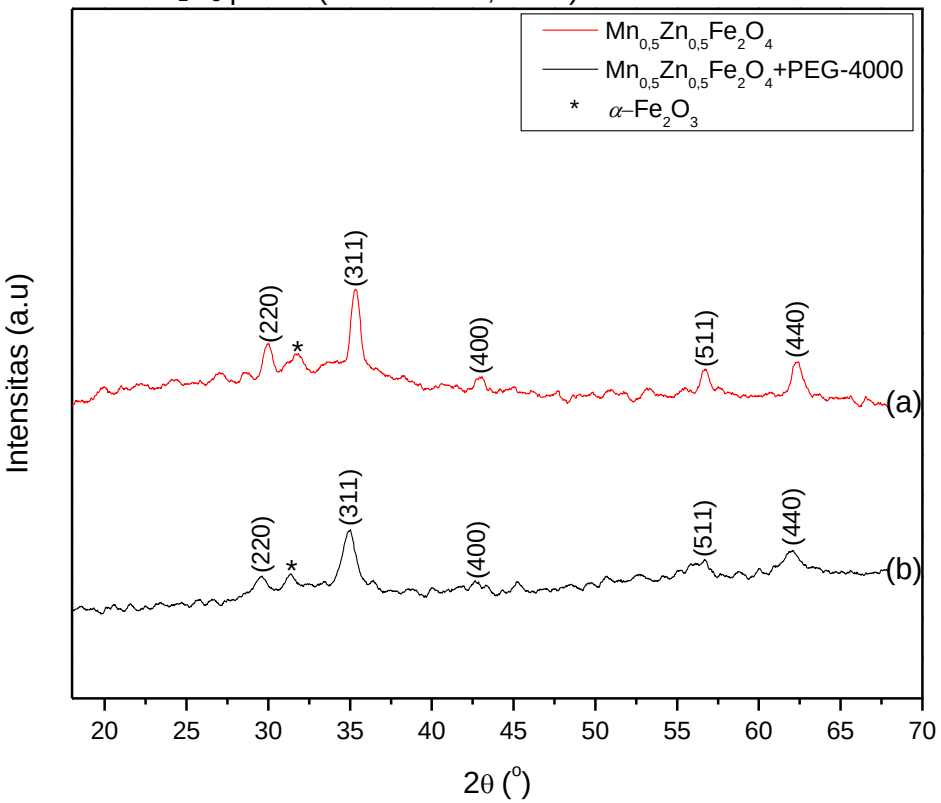

Figure 1. XRD pattern of $Mn_{0.5}Zn_{0.5}Fe_2O_4$ and $Mn_{0.5}Zn_{0.5}Fe_2O_4$+PEG-4000 nanoparticles

According to Table 3, the size of the crystal grains decreases after encapsulation. This decrease is because the nanoparticles are trapped in long PEG-4000 chains causing the movement of the particles to be blocked so that crystalline growth is inhibited. In addition, the microstrain and X-ray density did not change significantly after encapsulation.

Table 3. Data of lattice parameters, particles size, microstrain, and X-ray density of $Mn_{0.5}Zn_{0.5}Fe_2O_4$ and $Mn_{0.5}Zn_{0.5}Fe_2O_4$+PEG-4000

Sample	Lattice parameters (A)	Particles size (nm)	Microstrain	X-ray density (g/cm^3)
$Mn_{0.5}Zn_{0.5}Fe_2O_4$	8.42	27.8	0.016	5.25
$Mn_{0.5}Zn_{0.5}Fe_2O_4$+ PEG-4000 (50%)	8.51	19.1	0.024	5.08

The FTIR spectrum of $Mn_{0.5}Zn_{0.5}Fe_2O_4$ nanoparticles before and after encapsulated PEG-4000 is shown in Fig 2. In the FTIR spectrum $Mn_{0.5}Zn_{0.5}Fe_2O_4$ (Fig. 2a), there is an absorption peak at 3410.15 cm^{-1} which is a hydroxyl group (OH), 578.64 cm^{-1} are tetrahedral Fe-O groups and 447.20 cm^{-1} are Fe-O octahedral groups, each vibrating stretching [11, 12]. The FTIR spectrum of PEG-4000 (Fig. 2b) at 3441.00 cm^{-1}, 2878.00 cm^{-1}, 1465.00 cm^{-1}, 1342.46 cm^{-1}, 1281.00 cm^{-1}, 1249.00 cm^{-1}, 1103,28 cm^{-1}, 957,00 cm^{-1}, 840,96

cm^{-1} are the peaks of its absorption characteristics (Issa et al., 2011; Kareem et al., 2015). In the FTIR spectrum of PEG-4000 encapsulated $Mn_{0.5}Zn_{0.5}Fe_2O_4$ (Fig. 2c) there is also an absorption peak at 3410.15 cm^{-1} which is O-H stretching. The absorption peaks at 2885.51 cm^{-1}, 1281.00 cm^{-1}, 1249.00 cm^{-1}, 957.00 cm^{-1}, 840.96 cm^{-1} is stretching C-H, at 1465.00 cm^{-1}, 1342.46 cm^{-1} is C-H bending, at 1111.00 cm^{-1} is C-O-C stretching, at 570.93 cm^{-1} is M-O stretching in tetrahedral, and at 439.77 cm-1 and 362,62 cm^{-1} is M-O stretching in the octahedral (Issa et al., 2011; Kareem et al., 2015). The encapsulated $Mn_{0.5}Zn_{0.5}Fe_2O_4$ nanoparticles undergo changes in wavenumbers, this is because PEG-4000 is able to move the presence of water molecules on the nanoparticles.

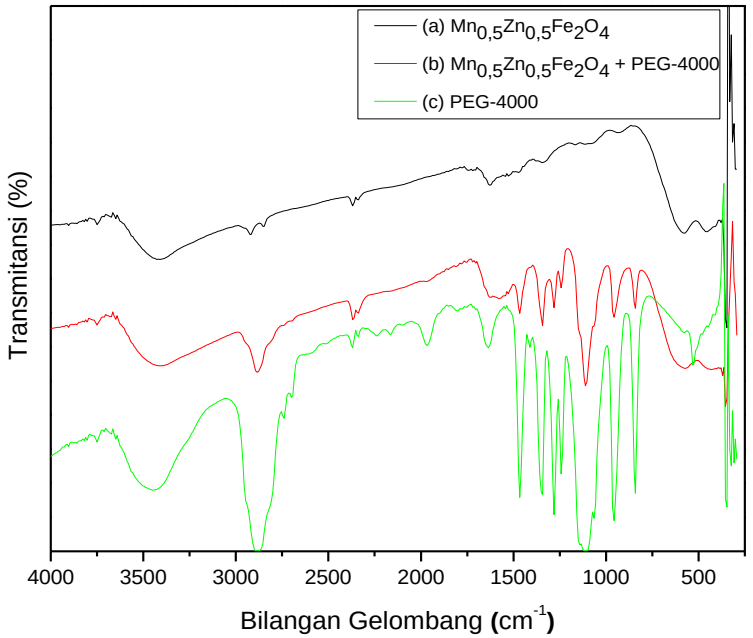

Figure 2. FTIR spectrum of (a) $Mn_{0.5}Zn_{0.5}Fe_2O_4$, (b) $Mn_{0.5}Zn_{0.5}Fe_2O_4$+PEG-4000, and (c) PEG-4000

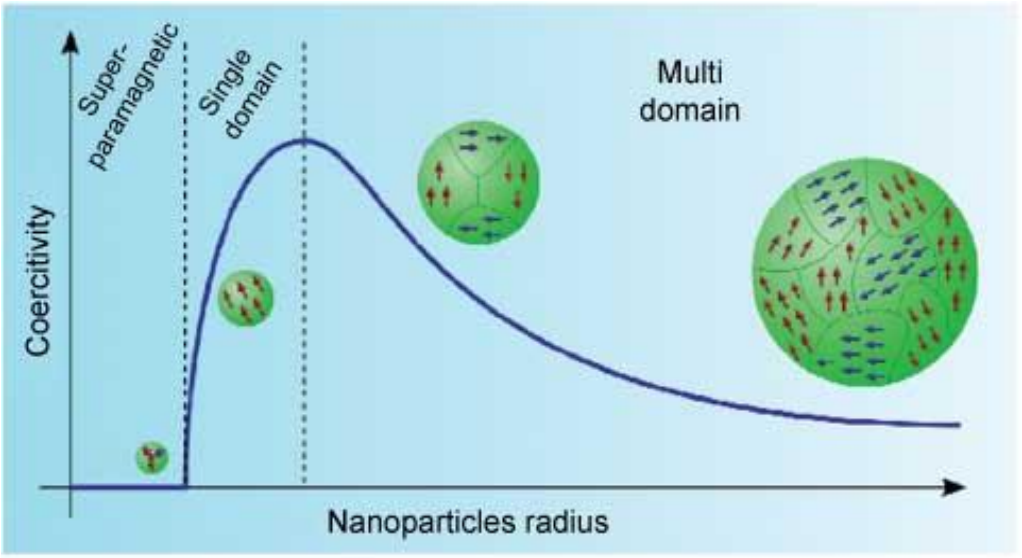

Figure 3. Schematic illustration of the coercivity-size relations of small particles

The results in Table 4 show that the coercive value tends to decrease with the smaller grain size after encapsulation. This indicates that all samples are in a single domain. The Magnetization (at H = 15 kOe), remanent magnetization, magnetic anisotropy constant decreased with increasing PEG-4000 concentration. This is due to PEG-4000 itself, where PEG-4000 is a non-magnetic material that weakens the magnetic properties of the sample (Nuzully et al., 2013).

Table 4. Magnetic properties of $Mn_{0.5}Zn_{0.5}Fe_2O_4$+PEG-4000 nanoparticles

Sample	PEG-4000 concentration (%)	H_c (Oe)	M (at H = 15 kOe) (emu/g)	M_r (emu/g)	K (erg/g)
M	0	47.6	10.4	1.4	495.0
A	25	46.7	10.4	0.2	485.4
B	33	49.1	10.4	0.3	510.5
C	50	45.8	10.3	0.3	472.7
D	67	45.0	8.3	0.2	372.8
E	75	47.5	9.5	0.4	452.4
F	80	47.5	7.2	0.4	343.7

$Mn_{0.5}Zn_{0.5}Fe_2O_4$+Silica nanoparticles

Based on XRD pattern $Mn_{0.5}Zn_{0.5}Fe_2O_4$ before and after encapsulated with silica (Figure 3), there are diffraction peaks (220), (311), (400), (511) and (440). The diffraction peaks are typical of the spinel ferrite plane. In addition, diffraction peaks (222) and SiO_2 phase are encapsulated as well. This occurs because of the effect of silica which is sufficient to form crystalline phase at low temperature and concentration so that it has the potential to form its own phase. Figure 4, also shows an angular shift of 2θ of the diffraction peak toward the right due to the nanoparticles being coated by silica, and indicating a decrease in spacing between plane (Martinez et al., 2006).

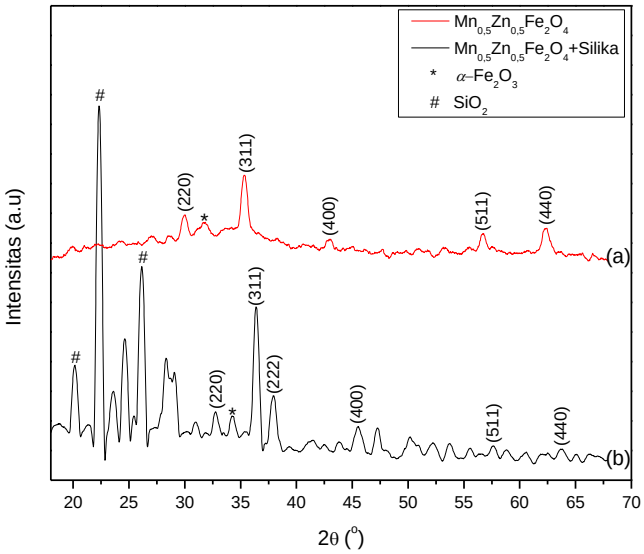

Figure 4. XRD pattern of $Mn_{0.5}Zn_{0.5}Fe_2O_4$ and $Mn_{0.5}Zn_{0.5}Fe_2O_4$+silica nanoparticles

Table 5 shows the grain size of crystals has increased from 27.8 nm to 32.8 nm. This is due to the effect of silica coating the nanoparticles. Changes in X-ray density and microstrain are insignificant after encapsulation.

Table 5. Data of lattice parameters, particles size, microstrain, and X-ray density of $Mn_{0.5}Zn_{0.5}Fe_2O_4$ and $Mn_{0.5}Zn_{0.5}Fe_2O_4$+silika

Sample	Lattice parameters (A)	Particles size (nm)	Microstrain	X-ray density (g/cm^3)
$Mn_{0.5}Zn_{0.5}FeO_4$	8.53	27.8	0.016	5.25
$Mn_{0.5}Zn_{0.5}Fe_2O_4$ +silika (50%)	8.18	32.8	0.013	5.72

The FTIR spectra of $Mn_{0.5}Zn_{0.5}Fe_2O_4$ before and after the encapsulated silica is shown in Figure 5. In the FTIR spectrum $Mn_{0.5}Zn_{0.5}Fe_2O_4$ (Figure 5a), there is an absorption peak at 3410.15 cm^{-1} representing OH group, at 578.64 cm^{-1} is the tetrahedral M-O, and at 447.20 cm^{-1} is M-O in octahedral, each vibrating stretching (Mandal et al., 2002; Baykal et al., 2014; Merdekani, 2013; Ui et al., 2009; Yan et al., 2004). In the FTIR spectrum of silica (Figure 5b) there is also an absorption at 3437.30 cm^{-1} which is O-H streatching. The absorption at

1087.85 cm^{-1} is Si-O-Si streatching (asymmetric), at 1065.00 cm^{-1} is Si-OH streatching, at 794.67 cm^{-1} is Si-O-Si streatching (symmetric), and at 471.00 cm^{-1} is Si-O-Si streatching stretching (Mandal et al., 2002; Baykal et al., 2014; Merdekani, 2013; Ui et al., 2009; Yan et al., 2004).

In the FTIR spectrum of silica encapsulated $Mn_{0.5}Zn_{0.5}Fe_2O_4$ (Figure 5c) shows the presence of typical silica and nanoparticle absorptions. The absorption at 3433.29 cm-1 was the O-H streatching group, at 2924.00 cm^{-1} and 2854.00 cm^{-1} is C-H streatching, at 1049.28 cm^{-1} is Si-O-Si streatching (asymmetric), at 964.41 cm^{-1} is Si-OH streatching, at 779.24 cm^{-1} is Si-O-Si streatching (symmetric), at 471.00 cm^{-1} is Si-O-Si streatching, at 570.93 cm^{-1} is M-O streatching in tetrahedral, and at 437.77 cm^{-1} and 362.62 cm^{-1} is stromalid M-O in octahedral stretching (Mandal et al., 2002; Baykal et al., 2014; Merdekani, 2013; Ui et al., 2009; Yan et al., 2004). The change in the encapsulated wavenumbers occurs because the nanoparticles have been coated by silica.

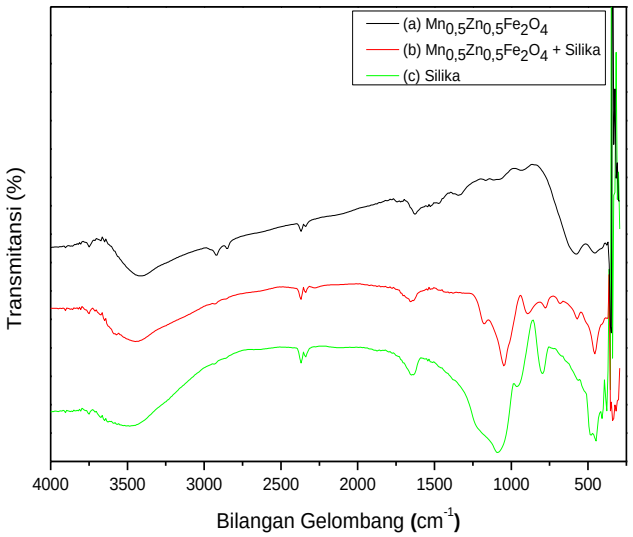

Figure 5. FTIR Spectrum of (a) $Mn_{0.5}Zn_{0.5}Fe_2O_4$, (b) $Mn_{0.5}Zn_{0.5}Fe_2O_4$+silica, and (c) Silica

The magnetic properties of $Mn_{0.5}Zn_{0.5}Fe_2O_4$ before and after encapsulation with silica are shown in Table 6. Table 6 shows the value of coercivity decreased with increasing silica concentration. Coercivity also depends heavily on the size of the grains of crystals where the size of the crystalline grains increases causing decreased coercivity (Akbarzadeh et al., 2012). This relationship shows the sample being in multi-domains. The presence of a diamagnetic phase of SiO_2 in nanoparticles also causes coercivity to decrease with increasing silica concentration. Magnetization (at H = 15 kOe), remanent magnetization, and magnetic anisotropy decreased with increasing silica concentration (Nadeem et al., 2014).

Table 6. Magnetic properties of $Mn_{0.5}Zn_{0.5}Fe_2O_4$+silica nanoparticles

Sample	Silica concentration (%)	H_c (Oe)	M (at H = 15 kOe) (emu/g)	M_r (emu/g)	K (erg/g)
M	0	47.6	10.4	1.4	495.0
P	5	47.5	7.7	1.2	365.3
Q	10	47.5	4.7	0.7	224.9
R	15	47.0	2.8	0.4	130.6
S	20	46.6	2.7	0.3	125.4
T	30	46.2	2.3	0.1	105.7
U	50	45.7	1.3	0.1	61.2

The encapsulation of $Mn_{0.5}Zn_{0.5}Fe_2O_4$ nanoparticles with varying concentrations of silica reveals significant changes in their magnetic properties, as shown in the table. Coercivity (Hc) demonstrates a slight decrease from 47.6 Oe for uncoated nanoparticles to 45.7 Oe at the highest silica concentration of 50%. This reduction is attributed to the increased separation between magnetic nanoparticles caused by the silica shell, which weakens dipolar interactions. The relatively stable coercivity across different silica

concentrations suggests that the encapsulation primarily affects surface interactions rather than the core magnetic domain structure, consistent with findings by Akbarzadeh et al. (2012).

Magnetization at H = 15 kOe (M) shows a substantial decrease from 10.4 emu/g for uncoated nanoparticles to 1.3 emu/g at 50% silica concentration. This sharp decline is due to the non-magnetic nature of silica, which dilutes the effective magnetic volume of the nanoparticles and reduces magnetic coupling. As silica concentration increases, the separation between nanoparticles grows, further diminishing their net magnetization. These results align with earlier studies that demonstrated weakened magnetic interactions following silica encapsulation (Nadeem et al., 2014).

A similar trend is observed in remanent magnetization (Mr), which decreases from 1.4 emu/g for uncoated nanoparticles to 0.1 emu/g at silica concentrations of 30% and 50%. This reduction reflects the significant disruption of long-range magnetic ordering caused by the insulating silica layer. With increasing silica content, fewer magnetic moments remain aligned after the removal of the external field, resulting in lower remanence.

The magnetic anisotropy constant (K) also declines dramatically, from 495.0 erg/g for uncoated nanoparticles to 61.2 erg/g at 50% silica concentration. This reduction indicates lower energy barriers for the realignment of magnetic moments, which can be attributed to decreased interparticle magnetic interactions and the non-magnetic contribution of the silica shell. Such behavior is consistent with prior findings that identified the insulating nature of silica as a factor in reducing exchange interactions within and between magnetic cores. Silica encapsulation enhances the stability and prevents agglomeration of $Mn_{0.5}Zn_{0.5}Fe_2O_4$ nanoparticles but leads to a significant trade-off in their magnetic properties. The moderate reduction in coercivity, combined with the sharp declines in magnetization, remanence, and anisotropy constant, underscores the impact of silica's non-magnetic nature and its role in increasing interparticle distance. These findings highlight the need to balance stability and magnetic performance when considering silica-encapsulated nanoparticles for applications in magnetic hyperthermia, drug delivery, and industrial catalysis.

CONCLUSION

$Mn_{0.5}Zn_{0.5}Fe_2O_4$ has been successfully synthesized and encapsulated by varying the concentration of encapsulation materials in the form of PEG-4000 and silica using coprecipitation method. The encapsulation results affect the characteristics of the crystal structure and magnetism properties of $Mn_{0.5}Zn_{0.5}Fe_2O_4$ nanoparticles in terms of grain size, morphology, functional groups, coercivity, and magnetization of the nanoperticles.

ACKNOWLEDGEMENT

The authors gratefully acknowledge the financial support provided by the Hibah Kompetensi (HIKOM) Kemenristek Dikti for the research conducted during the period 2015–2017. This funding facilitated comprehensive exploration and development of $Mn_{0.5}Zn_{0.5}Fe_2O_4$ nanoparticles, enabling advancements in synthesis methodologies and characterization techniques. The support from HIKOM was instrumental in acquiring advanced instrumentation, conducting extensive experimental studies, and fostering collaborative efforts to ensure the high quality of this research..

RECOMMENDATIONS

Further research is recommended to use variations in the concentration of encapsulation materials to obtain different and better results, because the encapsulation results affect the characteristics of the crystal structure and magnetic properties of nanoparticles.

REFERENCE

Abdullah, M. (2009). *Pengantar Nanosains*. ITB. Bandung.

Akbarzadeh, A., Samiei, M., & Davaran, S. (2012). Magnetic nanoparticles: preparation, physical properties, and applications in biomedicine, *Nanoscale Research Letters*, 7, pp. 144.

Al-Bermany, E., & Chen, B. (2020). Preparation and characterisation of poly(ethylene glycol)-adsorbed graphene oxide nanosheets. Polymer International, 70(3), 341-351. https://doi.org/10.1002/pi.6140

Al-husseny, W. H., Al-Sharuee, I. F., & Ali, B. R. (2023). Spectral and structural analysis for sodium silicate-based aerogel via normal drying pressure. Malaysian Journal of Science, 42(2), 47-55. https://doi.org/10.22452/mjs.vol42no2.7

Angermann, A., Hartmann, E., & Töpfer, J. (2010). Mixed-metal carbonates as precursors for the synthesis of nanocrystalline mn–zn ferrites. Journal of Magnetism and Magnetic Materials, 322(21), 3455-3459. https://doi.org/10.1016/j.jmmm.2010.06.044

Ashraf, M. A., Khan, A. M., Ahmad, M., & Sarfraz, M. (2015). Effectiveness of silica based sol-gel microencapsulation method for odorants and flavors leading to sustainable environment. Frontiers in Chemistry, 3. https://doi.org/10.3389/fchem.2015.00042

Baykal, A., Guner, S., Demira, A., Esira, S., & Genc, F. (2014). Effect of Zinc Substitution on Magneto-Optical Properties of $Mn_{1-x}Zn_xFe_2O_4/SiO_2$ Nanocomposites, *Ceramics International*, 40, pp. 13401–13408.

Ciriminna, R., & Pagliaro, M. (2013). Sol–gel microencapsulation of odorants and flavors: opening the route to sustainable fragrances and aromas. Chemical Society Reviews, 42(24), 9243. https://doi.org/10.1039/c3cs60286a

Dabagh, S., Haris, S. A., & Ertaş, Y. N. (2023). Engineered polyethylene glycol-coated zinc ferrite nanoparticles as a novel magnetic resonance imaging contrast agent. ACS Biomaterials Science &Amp; Engineering, 9(7), 4138-4148. https://doi.org/10.1021/acsbiomaterials.3c00255

Deraz, N. M., & Alarifi, A., (2012). Preparation and Characterization of Nano-Magnetic $Mn_{0.5}Zn_{0.5}Fe_2O_4$ System, *International Journal of Electrochemical Science*, 7, pp. 5828-5836.

Horvat, G., Pantić, M., Knez, Ž., & Novak, Z. (2019). Preparation and characterization of polysaccharide - silica hybrid aerogels. Scientific Reports, 9(1). https://doi.org/10.1038/s41598-019-52974-0

Iacoviță, C., Florea, A., Scorus, L., Páll, E., Dudric, R., Moldovan, A., & Lucaciu, C. M. (2019). Hyperthermia, cytotoxicity, and cellular uptake properties of manganese and zinc ferrite magnetic nanoparticles synthesized by a polyol-mediated process. Nanomaterials, 9(10), 1489. https://doi.org/10.3390/nano9101489

Issa, B., Qadri, S., Obaidat, I. M., Bowtell, R. W., & Haik, Y. (2011). PEG Coating Reduces NMR Relaxivity of $Mn_{0,5}Zn_{0,}5Gd_{0,02}Fe_{1,98}O_4$ Hyperthermia Nanoparticles, *Journal of Magnetic Resonance Imaging*, 34, pp. 1192-1198.

Kareem, S. H., Shamsuddin, M., & Lee, S. L. (2016). Effect of precipitation temperature on structural and magnetic features of polyethylene glycol-coated mn0.8zn0.2fe2 o 4 nanoparticles. Journal of Superconductivity and Novel Magnetism, 29(10), 2691-2697. https://doi.org/10.1007/s10948-016-3599-7

Kareem, S. H., Ati, A. A., Shamsuddin, M., & Lee, S. L. (2015). Nanostructural, Morphological and Magnetic Studies of $PEG/Mn_{(1-x)}Zn_{(x)}Fe_2O_4$ Nanoparticles Synthesized by Co-Precipitation, *Ceramics International*, 41, pp. 11702–11709.

Liu, C. P., Ming-Wei, L., Zhong, C., Juan-Ru, H., Yi-Ling, Ti., Tong, L., & Wen-Bo, M. (2007). Comparative Study of Magnesium Ferrite Nanocrystallites Prepared by Sol-Gel and Copresipitation Methods, *J Mater Sci*, 42, pp. 6133-6138.

Lu, A.H., Salabas, E. L., & Schuth, F. (2007). Magnetic Nanoparticles: Synthesis, Protection, Functionalization, and Application, *Angenwadte Chemistry of Sciences*, 46, pp.1222-1244.

Mandal, K., Chakraverty, S., Mandal, S. P., Agudo, P., Pal, M., & Chakravorty, D. (2002). Size-Dependent Magnetic Properties of $Mn_{0,5}Zn_{0,5}Fe_2O_4$ Nanoparticles in SiO_2 Matrix, *Journal of Applied Physics*, 92, pp. 501.

Martinez, J. R., Palomares-Sánchez, S. A., Ortega-Zarzosa, G., Ruiz, F., & Chumakov, Y. (2006). Rietveld Refinement of Amorphous SiO_2 Prepared Via Sol–Gel Method. *Materials Letters*, *60*(29-30), 3526-3529. https://doi.org/10.1016/j.matlet.2006.03.044

Matsumoto, M., Matsusaki, M., & Akashi, M. (2013). Preparation of biodegradable peptide nanospheres with hetero peg brush surfaces. Macromolecular Bioscience, 14(1), 142-150. https://doi.org/10.1002/mabi.201300201

Merdekani, S. (2013). Sintesis Partikel Nanokomposit Fe_3O_4/SiO_2 dengan Metode Kopresipitasi, *Prosiding Seminar Nasional Sains dan Teknologi Nuklir*,pp. 472-477.

Modak, S., Karan, S., Roy, S.K., Mukherjee, S., Das, D., & Chakrabarti, P.K. (2008). Preparation and Characterizations of SiO_2-Coated Nanoparticles of $Mn_{0,4}Zn_{0,6}Fe_2O_4$, *Journal of Magnetism and Magnetic Materials*, 321, pp. 169-174.

Nadeem, K., Zeb, F., Abid, M. A., Mumtaz, M., & Rehman, M. A. U. (2014). Effect of Amorphous Silica Matrix on Structural, Magnetic, and Dielectric Properties of Cobalt Ferrite/Silica Nanocomposites. *Journal of Non-Crystalline Solids*, *400*, 45–50. https://doi.org/10.1016/j.jnoncrysol.2014.05.004

Ngarajan, R., & Hatton, T. (2008). *Nanoparticles: Synthesis, Stabilization, Passivation, and Functionalization*. Washington DC: ADS.

Nuzully, S., Kato, T., Iwata, S., & Suharyadi, E. (2013). Pengaruh Konsentrasi Polyethylene Glycol (PEG) pada Sifat Kemagnetan Nanopartikel Magnetik PEG-Coated Fe_3O_4. *Jurnal Fisika Indonesia*, *17*(51), 35-40. https://doi.org/10.22146/jfi.24432

Patel, M., Park, J. K., & Jeong, B. (2023). Rediscovery of poly(ethylene glycol)s as a cryoprotectant for mesenchymal stem cells. Biomaterials Research, 27(1). https://doi.org/10.1186/s40824-023-00356-z

Sun, Y., Yan, C., Xie, J., Yan, D., Hu, K., Huang, S., & Xiong, F. (2019). High-performance worm-like mn–zn ferrite theranostic nanoagents and the application on tumor theranostics. ACS Applied Materials &Amp; Interfaces, 11(33), 29536-29548. https://doi.org/10.1021/acsami.9b08948

Ui, S. W., Lim, S. J., Lee, S. H., & Choi, S. C. (2009). Control of The Size and Morphology of Nano-Size Silica Particles Using a Sodium Silicate Solution, *Journal of Ceramic Processing Research*, 10, 4, pp. 553-558.

Wei, M., Guo, X., Qin, M., Pan, H., Cao, Y., & Wang, W. (2012). Mechanistic insights into the stabilization of srcsh3 by pegylation. Langmuir, 28(46), 16133-16140. https://doi.org/10.1021/la303466w

Widakdo, J., Istikhomah, N., Rifianto, A., Suharyadi, E., Kato, T., & Iwata, S. (2018). Crystal structures and magnetic properties of polyethylene glycol (peg-4000) encapsulated zn0.5ni0.5fe2o4 magnetic nanoparticles. Journal of Physics: Conference Series, 1011, 012068. https://doi.org/10.1088/1742-6596/1011/1/012068

Yacob, N. (2021). Effect of different molecular weight and concentration of polyethylene glycol (peg) on tensile and morphology of sago starch film. ASM Science Journal, 16, 1-10. https://doi.org/10.32802/asmscj.2021.571

Yan, S., Ling, W., & Zhou, E. (2004). Rapid synthesis of $Mn_{0.65}Zn_{0.35}Fe_2O_4/SiO_2$ homogeneous nanocomposites by modified sol–gel auto-combustion method, *Journal of Crystal Growth*, 273, pp. 226-233.

Zhang, D. E., Zhang, X.J., Zheng, H. G., & Yang. D. D. (2005). Synthesis and Characterization of $NiFe_2O_4$ Magnetic Nanorods via a PEG-Assisted Route, *Journal of Magnetism and Magnetic Materials*, 292, pp.79-82.

Zhang, H., Liu, M., Fan, H., & Zhang, X. (2012). Carbonated nano hydroxyapatite crystal growth modulated by poly(ethylene glycol) with different molecular weights. Crystal Growth &Amp; Design, 12(5), 2204-2212. https://doi.org/10.1021/cg200917y

Zhao, L., Yang, H., Cui, Y., Zhao, X., & Feng, S. (2007). Study of Preparation and Magnetic Properties of Silica-Coated Cobalt Ferrite Nanocomposites, *springer*, 42, pp. 4110-4114.